

## **PLANE WAVE SCATTERING FROM PERPENDICULARLY CROSSED MULTILAYERED STRIP GRATINGS**

A. Matsushima, T. L. Zinenko, H. Nishimori, and Y. Okuno

Department of Electrical and Computer Engineering  
Kumamoto University  
Kumamoto 860-8555, Japan

- 1. Introduction**
  - 2. Integral Equations**
  - 3. Moment Method**
  - 4. Power Relations**
  - 5. Numerical Results**
  - 6. Conclusion**
- Appendix. Evaluation of Inner Product**  
**References**

### **1. INTRODUCTION**

The electromagnetic wave scattering from infinite periodic gratings composed of strips or wires has been a classical topic in diffraction theory. One application of this structure is to use the property of wave absorption where the scatterers are not perfectly conducting but resistive type. From this viewpoint, the strip grating with one-dimensional periodicity has been treated by the method of Riemann-Hilbert boundary value problem [1] and the singular integral equation method [2, 3]. Here the use of approximate boundary conditions [4] enabled us to deal with the boundary value problems easily. The above methods both are based on so-called regularization procedure, so that they not only reduce the matrix size but also avoid the relative convergence [5] in numerical computations.

Two-dimensional gratings are more general structure and have been utilized as wave shielding/absorbing sheet [6–8], frequency selective

surfaces (FSS) [9, 10], and so on. Since shielding materials are arrangement of thin conducting fibers, the analyses have often performed by taking account of only the axial component of the conducting current [6, 7]. Although FSS treatments are mainly based on the full-wave theory using the vector modal functions [10], the above-mentioned regularization procedure is unfortunately difficult to achieve for such two-dimensional structures. Therefore in numerical computations we must choose the truncation numbers properly and carefully in order to obtain correct results.

The objective of the present paper is to apply the full-wave treatment to the multilayered strip gratings having crossed structure. This type is regarded as a microscopic model of electromagnetic wave absorbing sheet of the fiber type [8]. We treat both the axial and perpendicular components of the surface current on the strips. The boundary value problem is formulated into the set of integral equations, which is discretized to the linear equations by applying the moment method. Numerical computation is carried out for the distribution of the incident power to the reflected, transmitted, and absorbed powers. We direct our attention to the optimization of the grating parameters for maximizing the absorptivity. The equivalent circuit parameters of the crossed resistive grating will also be obtained.

The time dependence  $e^{j\omega t}$  is suppressed throughout this paper.

## 2. INTEGRAL EQUATIONS

As illustrated in Fig. 1, the grating planes composed of infinite periodic resistive strips are layered in vacuum with the constant interval  $h$  in the  $z$  direction. The number of the plane is  $Q$ . The width of the strips is  $2w$  and its period of allocation in each plane is  $d$  along the  $x$  and  $y$  axes alternatively. Assuming that the strips are thin enough compared with the wavelength and the skin depth of the strip medium, we impose the resistive type boundary conditions [4]

$$\left. \begin{aligned} \mathbf{E}_T|_{z=z_p+0} - \mathbf{E}_T|_{z=z_p-0} &= 0 \\ \frac{1}{2} [\mathbf{E}_T|_{z=z_p+0} + \mathbf{E}_T|_{z=z_p-0}] &= R \hat{z} \times [\mathbf{H}|_{z=z_p+0} - \mathbf{H}|_{z=z_p-0}] \\ &= R \mathbf{J}^{(p)} \end{aligned} \right\}$$

(on  $S_p$ ;  $p = 1, 2, \dots, Q$ ;  $z_p = (p-1)h$ ) (1)

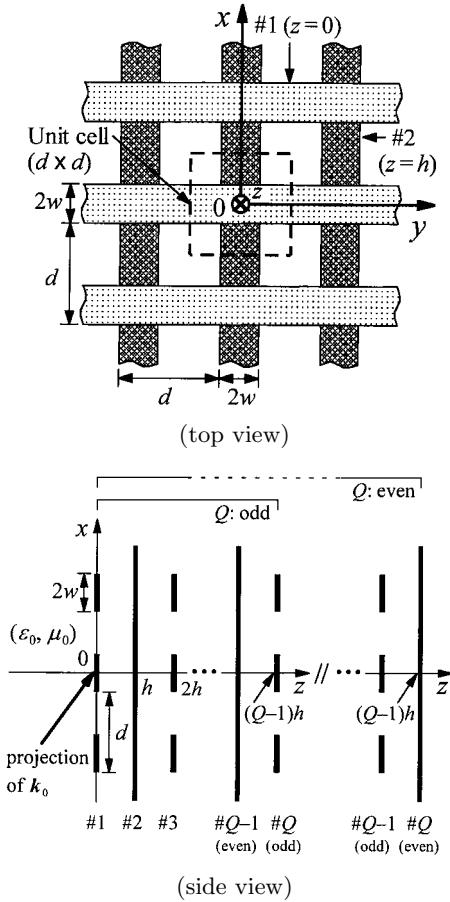


Figure 1. Geometry of the crossed strip grating.

where  $S_p$  is the strip region included in the unit cell

$$S_p = \begin{cases} \{(x, y, z_p) \mid -w < x < w, -d/2 < y < d/2\} & (p : \text{odd}) \\ \{(x, y, z_p) \mid -d/2 < x < d/2, -w < y < w\} & (p : \text{even}) \end{cases} \quad (2)$$

In (1),  $\hat{z}$  is the unit vector in the normal ( $z$ ) direction, and the subscript T denotes the transverse ( $xy$ ) components. The surface resistance  $R$  is defined by

$$R = \begin{cases} 1/[j\omega\epsilon_0\tau(\epsilon_r - 1) + \tau\sigma] & (\text{lossy dielectric}) \\ 1/[j\omega\epsilon_0\tau(\epsilon_r - 1)] & (\text{pure dielectric; } \sigma = 0) \\ 1/(\tau\sigma) & (\text{resistive; } \omega\epsilon_0\epsilon_r \ll \sigma) \\ 0 & (\text{perfectly conducting; } \sigma \rightarrow \infty) \end{cases} \quad (3)$$

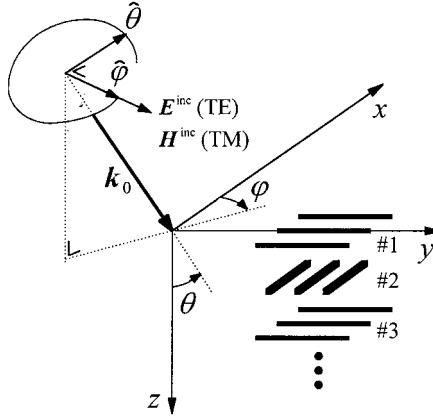


**Figure 2.** Incident plane wave.

where  $\varepsilon_r$ ,  $\sigma$ , and  $\tau$  are the relative permittivity, conductivity, and thickness of the strips, respectively. The function  $\mathbf{J}^{(q)}$  stands for the density of conducting current (polarization current) if  $R$  is pure real (pure imaginary).

The incident plane wave is illustrated with Fig. 2. The propagation vector  $\mathbf{k}_0$  makes an angle  $\theta$  with respect to the grating normal, and its projection onto the transverse ( $xy$ ) plane is inclined from the  $x$  axis by an angle  $\varphi$ . We classify the electromagnetic field into the TE and TM modes in which the electric and magnetic fields, respectively, are parallel with the transverse plane.

Let us express the total field by the sum of the incident and scattered fields as

$$(\mathbf{E}, \mathbf{H}) = (\mathbf{E}^{\text{inc}}, \mathbf{H}^{\text{inc}}) + \sum_{p=1}^Q (\mathbf{E}^{\text{sc}(p)}, \mathbf{H}^{\text{sc}(p)}) \quad (4)$$

The superscript  $\text{sc}(p)$  denotes the scattered field due to the induced current on the strips  $S_p$ . The transverse components of the incident and scattered fields are

$$\begin{bmatrix} \mathbf{E}_T^{\text{inc}} \\ \mathbf{H}_T^{\text{inc}} \end{bmatrix} = \iota_\tau \begin{bmatrix} \Psi_{\tau 00} \\ \eta_{\tau 00} \hat{z} \times \Psi_{\tau 00} \end{bmatrix} e^{-j\gamma_{00}z} \quad (5)$$

$$\iota_\tau = \begin{cases} -1 & (\tau = 1; \text{TE-inc.}) \\ \cos \theta & (\tau = 2; \text{TM-inc.}) \end{cases} \quad (6)$$

$$\begin{bmatrix} \mathbf{E}_T^{\text{sc}(p)} \\ \mathbf{H}_T^{\text{sc}(p)} \end{bmatrix} = \sum_{i=-\infty}^{\infty} \sum_{l=-\infty}^{\infty} \sum_{t=1}^2 \rho_{til}^{(p)} \begin{bmatrix} \Psi_{til} \\ \mathbf{\Psi}_{til} \end{bmatrix} e^{-j\gamma_{il}|z-z_p|} \quad (7)$$

The amplitude of the incident electric field is taken as  $1/d$ , and the set of  $\rho_{til}^{(p)}$  is the unknown coefficients of the TE ( $t = 1$ ) and TM ( $t = 2$ ) scattered modes. In (5) and (7) we used the vector modal functions defined by [10]

$$\begin{bmatrix} \Psi_{1il} \\ \Psi_{2il} \end{bmatrix} = V_{il} \begin{bmatrix} \beta_l \hat{x} - \alpha_i \hat{y} \\ \alpha_i \hat{x} + \beta_l \hat{y} \end{bmatrix} e^{-j(\alpha_i x + \beta_l y)}, \quad V_{il} = \frac{1}{d\sqrt{\alpha_i^2 + \beta_l^2}} \quad (8)$$

where the propagation constants and modal admittances are

$$\begin{cases} \alpha_i = k_0 \sin \theta \cos \varphi + 2i\pi/d \\ \beta_l = k_0 \sin \theta \sin \varphi + 2l\pi/d \\ \gamma_{il} = (k_0^2 - \alpha_i^2 - \beta_l^2)^{1/2} \quad (\text{Im } \gamma_{il} \leq 0) \end{cases} \quad (9)$$

$$\eta_{1il} = \gamma_{il}/(k_0 \zeta_0), \quad \eta_{2il} = k_0/(\zeta_0 \gamma_{il}) \quad (10)$$

with  $k_0 = \omega\sqrt{\varepsilon_0\mu_0} = 2\pi/\lambda_0$ ,  $\zeta_0 = \sqrt{\mu_0/\varepsilon_0}$ . Note that the modal function (8) satisfies the periodicity condition, for any component  $\Psi$ , that  $\Psi(x + md, y + nd) = \Psi(x, y)e^{-j(\alpha_0 md + \beta_0 nd)}$ . Note that the following orthonormal condition holds

$$\int_{-d/2}^{d/2} \int_{-d/2}^{d/2} \Psi_{til} \cdot \overline{\Psi_{t'i'l'}} dx dy = \delta_{tt'} \delta_{ii'} \delta_{ll'} \quad (11)$$

where the overline denotes complex conjugate, and the symbol  $\delta_{mn}$  stands for Kronecker's delta.

Applying (7) into (1), we can write the induced surface current density on  $S_p$  in terms of the modal coefficients as

$$\mathbf{J}^{(p)} = -2 \sum_{i=-\infty}^{\infty} \sum_{l=-\infty}^{\infty} \sum_{t=1}^2 \rho_{til}^{(p)} \eta_{til} \mathbf{\Psi}_{til} \quad (12)$$

Fourier analysis of (12) over the unit cell and the absence of  $\mathbf{J}^{(p)}$  on the gaps lead us to the integral representation of the coefficients

$$\rho_{til}^{(p)} = -\frac{1}{2\eta_{til}} \int_{S_p} \mathbf{J}^{(p)} \cdot \overline{\mathbf{\Psi}_{til}} dS \quad (13)$$

The expressions (4), (5), (7), and (13) are combined and substituted into the resistive boundary condition  $\mathbf{E} = R\mathbf{J}^{(p)}$  in (1). Thus we arrive at the set of integral equations

$$R\mathbf{J}^{(p)} + \sum_{q=1}^Q \sum_{i=-\infty}^{\infty} \sum_{l=-\infty}^{\infty} \sum_{t=1}^2 \frac{1}{2\eta_{til}} \Psi_{til} \int_{S_q} \mathbf{J}^{(q)} \cdot \overline{\Psi_{til}} dS e^{-j\gamma_{il}|z_p - z_q|} = \iota_{\tau} \Psi_{\tau 00} e^{-j\gamma_{00}z_p} \quad (\text{on } S_p, p = 1, 2, \dots, Q) \quad (14)$$

### 3. MOMENT METHOD

In the neighborhood of the edge of resistive strips, the surface current that flows along the edge (toward the edge) approaches a nonzero constant (vanishes) [11]. Taking account of this, we approximate the unknown functions as

$$\mathbf{J}^{(p)} \approx \frac{1}{\zeta_0} \sum_{s=1}^2 \sum_{m=M_{ps}^-}^{M_p^+} \sum_{n=N_{ps}^-}^{N_p^+} f_{smn}^{(p)} \Phi_{smn}^{(p)} \quad (15)$$

where the truncation numbers are

$$M_{ps}^- = \begin{cases} 0 & (p : \text{odd}, s = 1) \\ 1 & (p : \text{odd}, s = 2) \\ -N_{\parallel} & (p : \text{even}) \end{cases} \quad M_p^+ = \begin{cases} N_{\perp} & (p : \text{odd}) \\ N_{\parallel} & (p : \text{even}) \end{cases} \quad (16)$$

$$N_{ps}^- = \begin{cases} -N_{\parallel} & (p : \text{odd}) \\ 0 & (p : \text{even}, s = 1) \\ 1 & (p : \text{even}, s = 2) \end{cases} \quad N_p^+ = \begin{cases} N_{\parallel} & (p : \text{odd}) \\ N_{\perp} & (p : \text{even}) \end{cases} \quad (17)$$

and the basis functions are

$$\begin{bmatrix} \Phi_{1mn}^{(p)} \\ \Phi_{2mn}^{(p)} \end{bmatrix} = \begin{cases} U_{mn}^{(1)} \begin{bmatrix} j\beta_n \hat{y} & \frac{m\pi}{2w} \hat{x} \\ \frac{m\pi}{2w} \hat{y} & j\beta_n \hat{x} \end{bmatrix} \begin{bmatrix} \cos \frac{m\pi(x-w)}{2w} \\ \sin \frac{m\pi(x-w)}{2w} \end{bmatrix} e^{-j\beta_n y} & (p : \text{odd}) \\ U_{mn}^{(2)} \begin{bmatrix} j\alpha_m \hat{x} & \frac{n\pi}{2w} \hat{y} \\ \frac{n\pi}{2w} \hat{x} & j\alpha_m \hat{y} \end{bmatrix} \begin{bmatrix} \cos \frac{n\pi(y-w)}{2w} \\ \sin \frac{n\pi(y-w)}{2w} \end{bmatrix} e^{-j\alpha_m x} & (p : \text{even}) \end{cases} \quad (18)$$

with the normalizing factors

$$\begin{cases} U_{mn}^{(1)} = \sqrt{\frac{w/d}{(1 + \delta_{m0}) [(m\pi/2)^2 + (\beta_n w)^2]}} \\ U_{mn}^{(2)} = \sqrt{\frac{w/d}{(1 + \delta_{n0}) [(\alpha_m w)^2 + (n\pi/2)^2]}} \end{cases} \quad (19)$$

The set of functions (18) is the transverse field of the orthogonal modes in the parallel plate waveguide having the plate spacing  $2w$ , and therefore satisfies the orthonormal condition

$$\int_{S_p} \Phi_{smn}^{(p)} \cdot \overline{\Phi_{\sigma\mu\nu}^{(p)}} dS = \delta_{s\sigma} \delta_{m\mu} \delta_{n\nu} \quad (20)$$

After the expansion (15) is substituted into the integral equations (14), the Galerkin procedure is used to discretize the system of equations.

We take the inner product of the both sides with  $\Phi_{\sigma\mu\nu}^{(p)}$  and integrate them over the area of strips  $S_p$ . Making use of the orthonormality (20) and the symbol for the inner product

$$C_{smn,til}^{(p)} = \int_{S_p} \Phi_{smn}^{(p)} \cdot \overline{\Psi_{til}} dS \quad (21)$$

we are led to the set of the simultaneous linear algebraic equations

$$\begin{aligned} \frac{R}{\zeta_0} f_{\sigma\mu\nu}^{(p)} + \sum_{q=1}^Q \sum_{s=1}^2 \sum_{m=M_{qs}^-}^{M_q^+} \sum_{n=N_{qs}^-}^{N_q^+} K_{\sigma\mu\nu,smn}^{(pq)} f_{smn}^{(q)} = G_{\sigma\mu\nu}^{(p)} \\ (p = 1, 2, \dots, Q; \sigma = 1, 2; \mu = M_{p\sigma}^-, M_{p\sigma}^- + 1, \dots, M_p^+; \\ \nu = N_{p\sigma}^-, N_{p\sigma}^- + 1, \dots, N_p^+) \end{aligned} \quad (22)$$

where the matrix elements are represented by

$$K_{\sigma\mu\nu,smn}^{(pq)} = \sum_{i=-L}^L \sum_{l=-L}^L e^{-j\gamma_{il}|z_p - z_q|} \sum_{t=1}^2 \frac{1}{2\zeta_0 \eta_{til}} \overline{C_{\sigma\mu\nu,til}^{(p)}} C_{smn,til}^{(q)} \quad (23)$$

$$G_{\sigma\mu\nu}^{(p)} = e^{-j\gamma_{00}z_p} \overline{\nu_\tau C_{\sigma\mu\nu,\tau 00}^{(p)}} \quad (24)$$

The infinite sums in (23) are truncated at  $i, l = \pm L$  for the numerical computation. See Appendix for the analytical evaluation of the inner product (21).

After (22) is solved numerically to obtain the coefficients  $f_{smn}^{(p)}$ , we can compute the modal coefficients by

$$\rho_{til}^{(p)} = -\frac{1}{2\zeta_0\eta_{til}} \sum_{s=1}^2 \sum_{m=M_{ps}^-}^{M_p^+} \sum_{n=N_{ps}^-}^{N_p^+} f_{smn}^{(p)} C_{smn,til}^{(p)} \quad (25)$$

which is derived from (13), (15), and (21).

#### 4. POWER RELATIONS

The incident, reflected, and transmitted powers are obtained by integrating the normal component of the Poynting vector  $\hat{z} \cdot \text{Re}(\mathbf{E} \times \overline{\mathbf{H}})$  over the transverse plane for unit cell:  $|x| < d/2$ ,  $|y| < d/2$ , and  $z = \text{constant}$ . From (5) the incident power is found to be  $\eta_{\tau 00} \iota_{\tau}^2$ . Computing the reflected and transmitted powers from (7) and normalizing them by the incident one, we can express the relative reflected and transmitted powers for each mode as

$$\begin{cases} P_{til}^{\text{ref}} = \frac{\eta_{til}}{\eta_{\tau 00}} \left| \frac{1}{\iota_{\tau}} \sum_{p=1}^Q \rho_{til}^{(p)} e^{-j\gamma_{il}z_p} \right|^2 \\ P_{til}^{\text{tr}} = \frac{\eta_{til}}{\eta_{\tau 00}} \left| \delta_{t\tau} \delta_{i0} \delta_{l0} + \frac{1}{\iota_{\tau}} \sum_{p=1}^Q \rho_{til}^{(p)} e^{j\gamma_{il}z_p} \right|^2 \end{cases} \quad (26)$$

The absorbed power that is dissipated inside the strips is obtained by integrating  $R|\mathbf{J}^{(p)}|^2$  on the strips. Using (15) and (20), we have its normalized value as

$$\begin{aligned} P^{\text{abs}} &= \frac{1}{\eta_{\tau 00} \iota_{\tau}^2} \sum_{p=1}^Q \int_{S_p} R |\mathbf{J}^{(p)}|^2 dS \\ &= \frac{R}{\zeta_0^2 \eta_{\tau 00} \iota_{\tau}^2} \sum_{p=1}^Q \sum_{s=1}^2 \sum_{m=M_{ps}^-}^{M_p^+} \sum_{n=N_{ps}^-}^{N_p^+} \left| f_{smn}^{(p)} \right|^2 \end{aligned} \quad (27)$$

The powers evaluated above must satisfy the conservation law

$$\sum_{t=1}^2 \sum_{\substack{i,l \\ (\text{Re } \gamma_{il} > 0)}} \left( P_{til}^{\text{ref}} + P_{til}^{\text{tr}} \right) + P^{\text{abs}} = 1 \quad (28)$$

The energy error is defined by the absolute value of the difference between both sides of (28).

## 5. NUMERICAL RESULTS

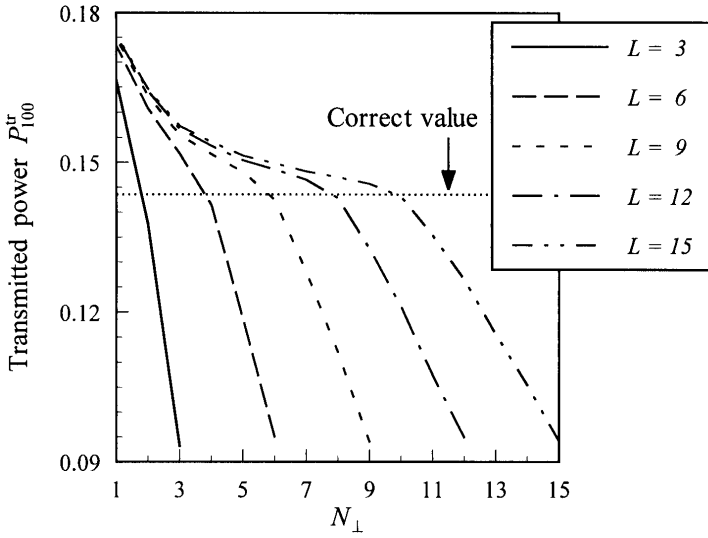
Since the energy error is always less than machine epsilon in the present numerical scheme, we must examine the behavior of physical values as the truncation numbers are changed. Accuracy and efficiency in numerical computations are much influenced by the choice of three truncation numbers  $N_{\perp}$ ,  $N_{\parallel}$ , and  $L$ . In Fig. 3(a) we show the dependence of the transmitted power on  $N_{\perp}$  for fixed  $N_{\parallel}$  and the parameter  $L$ . The power first converges to the stable value at some critical number of  $N_{\perp}$ , and then diverges. This is a typical behavior of the relative convergence phenomenon [5], and this stable value is considered to lie near the true value. From this we can set the criterion for  $N_{\perp}$  as

$$N_{\perp} = \left\lceil \frac{2w}{d}(2L + 1) \right\rceil \quad (29)$$

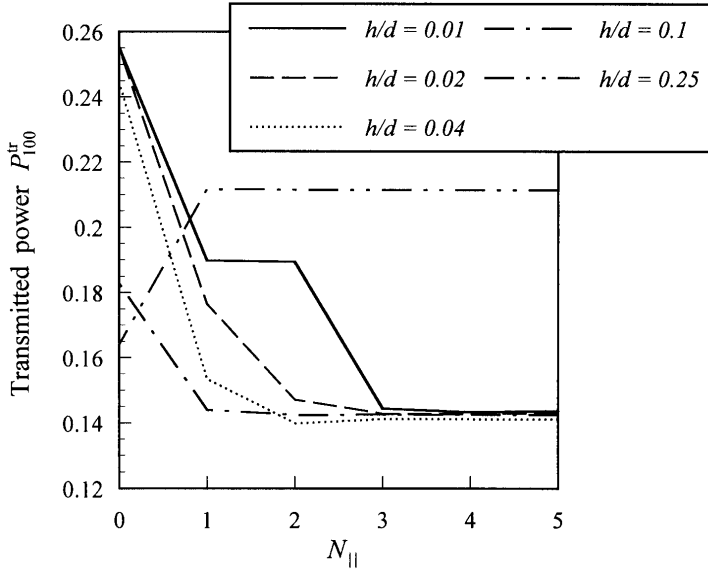
where  $\lceil x \rceil$  is an integer not exceeding  $x$ . In this figure the proper value of  $N_{\perp}$  is 2, 4, 6, 8, and 10 for  $L = 3, 6, 9, 12,$  and  $15$ , respectively.

Figure 3(b) shows the convergence of the transmitted power for the different values of the layer distance  $h/d$ . If the grating planes lie apart ( $h/d > 0.1$ ),  $N_{\parallel} = 2$  is enough. But for closed gratings the value of  $N_{\parallel}$  should be more, because we have larger variation in the surface current density due to the interaction among the planes.

In Fig. 4 the comparison is given for the transmission coefficients between two types of perfectly conducting gratings: strips and wires [6]. The wires are assumed to have the equivalent radius, i.e., a quarter of the strip width [12]. Since the scatterers are extremely thin with respect to the wavelength, it is enough to take into account the axial current only ( $N_{\perp} = 0$ ). However the truncation number  $L$  must be large to yield correct convergence; (29) is no longer applicable to such a small value of  $2w/d$ . The transmission coefficient [6] for co- and



(a)



(b)

**Figure 3.** Convergence of the relative transmitted power of the copolarized dominant mode for TE-incidence. The parameters are  $Q = 2$ ,  $2w/d = 1/3$ ,  $R = 0$  (perfectly conducting),  $d/\lambda_0 = 1.5$ ,  $\theta = 15^\circ$ , and  $\varphi = 45^\circ$ . (a)  $h/d = 0.1$ ,  $N_{\parallel} = 2$ , (b)  $N_{\perp} = 6$ ,  $L = 9$ .

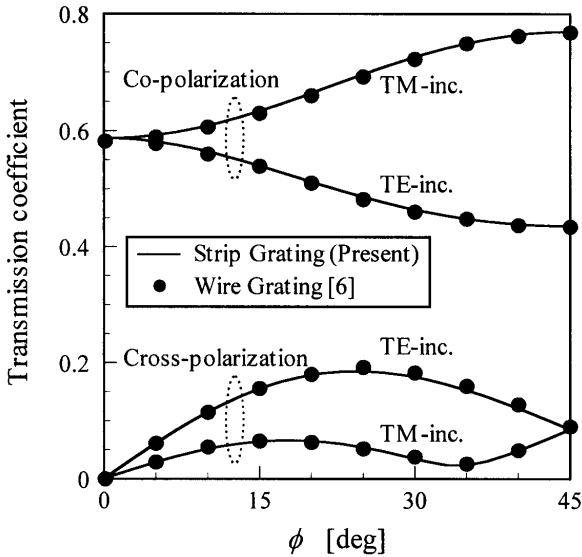
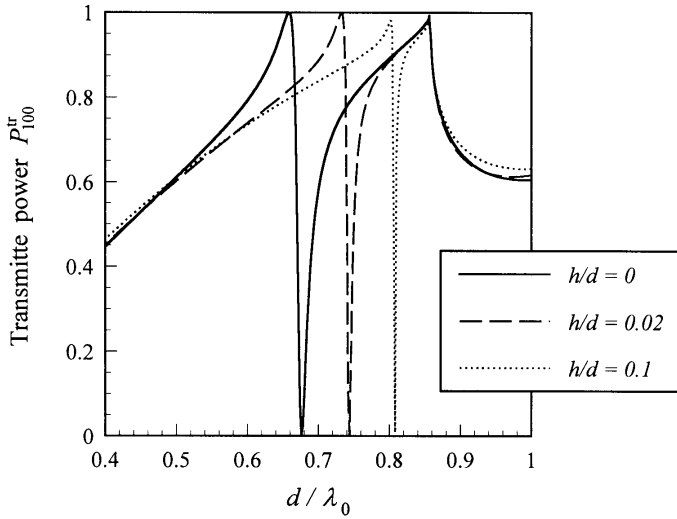


**Figure 4.** Comparison of the transmission coefficients with the crossed wire grid [6] having the equivalent wire radius  $w/2$ . The parameters are  $Q = 2$ ,  $h/d = 1$ ,  $2w/d = 0.004$ ,  $R = 0$  (perfectly conducting),  $d/\lambda_0 = 0.1$ , and  $\theta = 45^\circ$ . The truncation numbers are  $N_\perp = 0$ ,  $N_\parallel = 1$ , and  $L = 150$ .

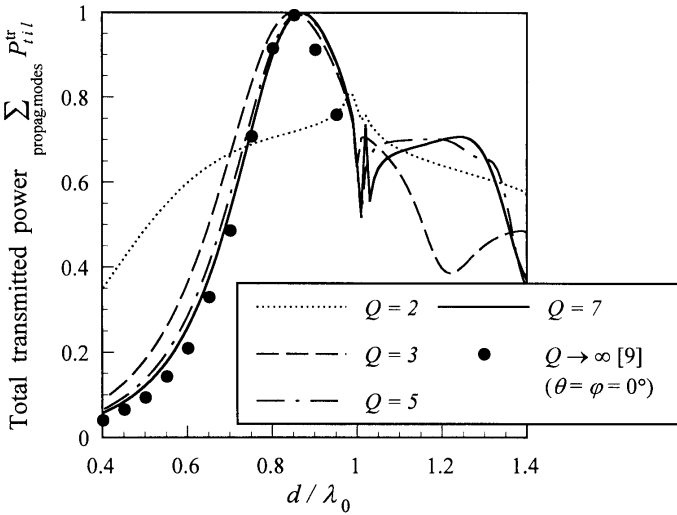
cross-polarization is defined by  $E_\varphi^{\text{tr}}/E_\varphi^{\text{inc}}$  and  $E_\theta^{\text{tr}}/E_\varphi^{\text{inc}}$ , respectively, at TE-incidence. In the case of TM-incidence, it is defined by  $E_\theta^{\text{tr}}/E_\theta^{\text{inc}}$  and  $E_\varphi^{\text{tr}}/E_\theta^{\text{inc}}$ . We have very good agreement between the strip and wire gratings.

Figure 5 shows the frequency characteristics of the transmitted power for perfectly conducting gratings. Figure 5(a) concerns the double-layered crossed gratings at  $h/d = 0.02$  and  $0.1$ , and the periodic square apertures perforated in a conducting screen ( $h/d = 0$ ). The latter case was treated independently based on FSS analysis [10]. We observe that the strong resonance shifts to high frequencies as the distance  $h/d$  increases. The common peak at  $d/\lambda_0 \approx 0.858$  concerns Wood’s anomaly where the degenerated higher order modes  $((i, l) = (0, -1), (-1, 0))$  begin to propagate.

Figure 5(b) is obtained under the condition that the thickness of the multilayered grating, i.e., the distance between two outermost grating planes, is fixed. We set the incidence almost normal, because the computation at exactly normal incidence involves division by zero



(a)



(b)

**Figure 5.** Frequency dependence of the relative transmitted power for TE-incidence. The strips are perfectly conducting ( $R = 0$ ). (a) Co-polarized dominant mode.  $2w/d = 0.2$ ,  $Q = 2$ ,  $\theta = 15^\circ$ , and  $\varphi = 45^\circ$ , (b) Total power.  $2w/d = 0.3$ ,  $(Q - 1)h/d = 0.2$ , and  $\theta = \varphi = 1^\circ$ .

without special analytical preparation. Total transmission occurs at  $d/\lambda_0 \approx 0.86$  except for the double-layered grating. The circular marks for  $Q \rightarrow \infty$  correspond to the periodic square apertures in a thick conducting screen at normal incidence [9]. The curve approaches the set of marks as  $Q$  is increased.

Figure 6 shows the absorbing rate  $P^{\text{abs}}$  (in %) of the double-layered crossed grating. There is no absorption on the abscissa  $2w/d = 0$  that corresponds to the absence of strips. The values for  $2w/d \approx 1$  are predicted by those of an infinite plane sheet with the halved resistance  $R/\zeta_0 = 1/2$ , that is,  $P^{\text{abs}} = 2 \cos \theta / (1 + \cos \theta)^2$ . The values based on this formula is about 50.0%, 44.4%, and 32.7% at  $\theta = 0^\circ$ ,  $60^\circ$ , and  $75^\circ$ , respectively, which is found to be good approximation for both polarizations. Note that the 49%-contour for TE-incidence extends to the region of small  $2w/d$  and large  $\theta$ . Simple analysis tells us that the relative absorbed power never exceeds 50% by using such a resistive sheet with negligible electrical thickness.

Figure 7 presents the absorbing rate of the 6-layered grating as a function of the layer distance  $h/d$  and the surface resistance  $R/\zeta_0$ . The valley and hills appear alternatively with an approximate period  $h/d \approx 0.6$ . This periodicity stems from the mode interaction among the strip layers. The hills are predicted by  $h \cos \theta / \lambda_0 \approx (\nu - 1)/4$  with  $\nu$  being a positive integer. The maximum of absorption is about 94% at optimized parameters.

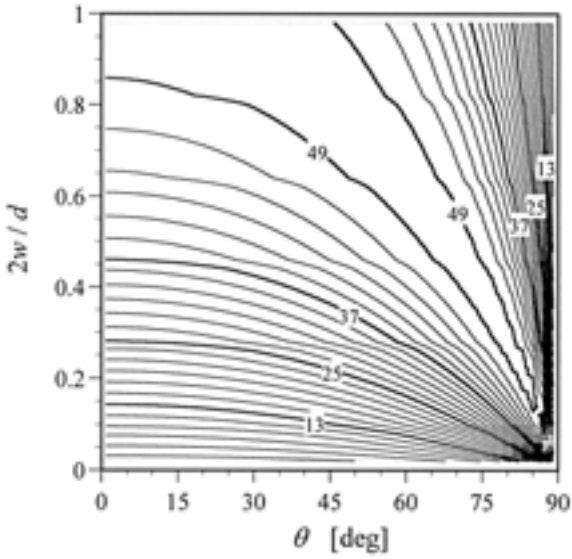
Figure 8 shows the equivalent impedance of the double-layered crossed grating for very small  $h/d$  and  $\varphi$  as a function of wavelength. With regard to the equivalent circuit in Fig. 9, the impedance is defined by

$$\frac{Z}{\zeta_0} = \begin{cases} -(1 + \rho)/(2\rho \cos \theta) & \text{(TE-inc.)} \\ -(1 + \rho) \cos \theta / (2\rho) & \text{(TM-inc.)} \end{cases} \quad (30)$$

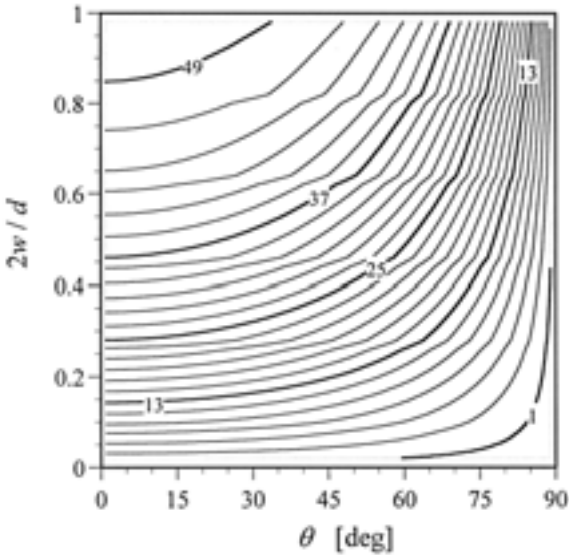
where the reflection coefficient  $\rho$  is defined by

$$\rho = \begin{cases} E_\varphi^{\text{ref}} / E_\varphi^{\text{inc}} & \text{(TE-inc.)} \\ E_\theta^{\text{ref}} / E_\theta^{\text{inc}} & \text{(TM-inc.)} \end{cases} \quad (31)$$

In Fig. 8, the value of  $Z/\zeta_0$  at the low frequency limit is  $2 + 0j$  as expected. The real part decreases monotonically as the frequency increases, but that the imaginary part has a extreme at  $d/\lambda_0 \approx 0.03$ . This result is inconsistent with the widely accepted idea that the reactance is negligibly small at the quasi-static region. We also see that, at low frequencies, the curves are almost independent of the incident



(a)



(b)

**Figure 6.** Dependence of the relative absorbed power  $P^{\text{abs}}$  (in %) on the incident angle and the strip width. The parameters are  $Q = 2$ ,  $h/d = 0.01$ ,  $R/\zeta_0 = 1$ ,  $d/\lambda_0 = 0.2$ , and  $\varphi = 1^\circ$ . (a) TE-incidence, (b) TM-incidence.

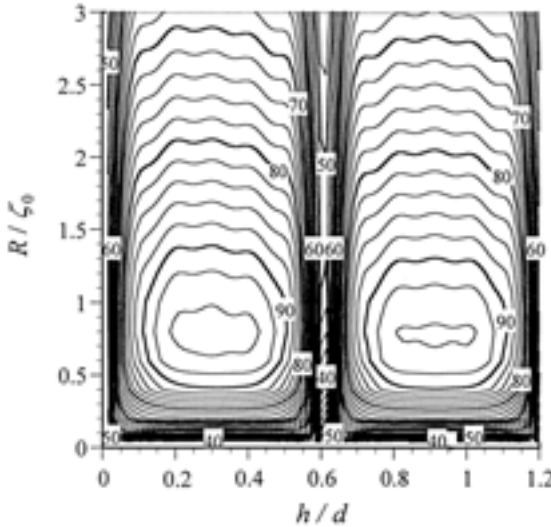


**Figure 7.** Dependence of the relative absorbed power  $P^{\text{abs}}$  (in %) on the layer distance and the surface resistance for TM-incidence. The parameters are  $Q = 6$ ,  $2w/d = 0.65$ ,  $d/\lambda_0 = 0.85$ ,  $\theta = 15^\circ$ , and  $\varphi = 45^\circ$ .

angle and the polarization. The circular marks are added for reference, which are computed by the a simple parallel connection formula

$$Z = Z_E Z_H / (Z_E + Z_H) \tag{32}$$

where  $Z_E$  ( $Z_H$ ) is the equivalent impedance of one-dimensional grating at E-wave (H-wave) incidence [1, 3]

$$\begin{cases} \frac{Z_E}{\zeta_0} = \frac{d}{2w} \cdot \frac{R}{\zeta_0} + j \frac{d}{\lambda_0} S \left( \frac{2\pi w}{d} \right) \\ \frac{Z_H}{\zeta_0} = \frac{16d}{3\pi^2 w} \cdot \frac{R}{\zeta_0} - j \left( \frac{4d}{\lambda_0} \log \csc \frac{\pi w}{d} \right)^{-1} \end{cases} \tag{33}$$

with  $S(x) = \sum_{l=1}^{\infty} \sin^2(lx)/l^3$ . Because the interaction of higher order modes is not taken into account, it is natural that the marks are not so accurate. However this comparison is quite suggestive to interpret the behavior of the impedance curves. Since numerical computations for the gratings of more than ten layers cost much CPU time and memory storage, the above formula is useful in treating such structures.

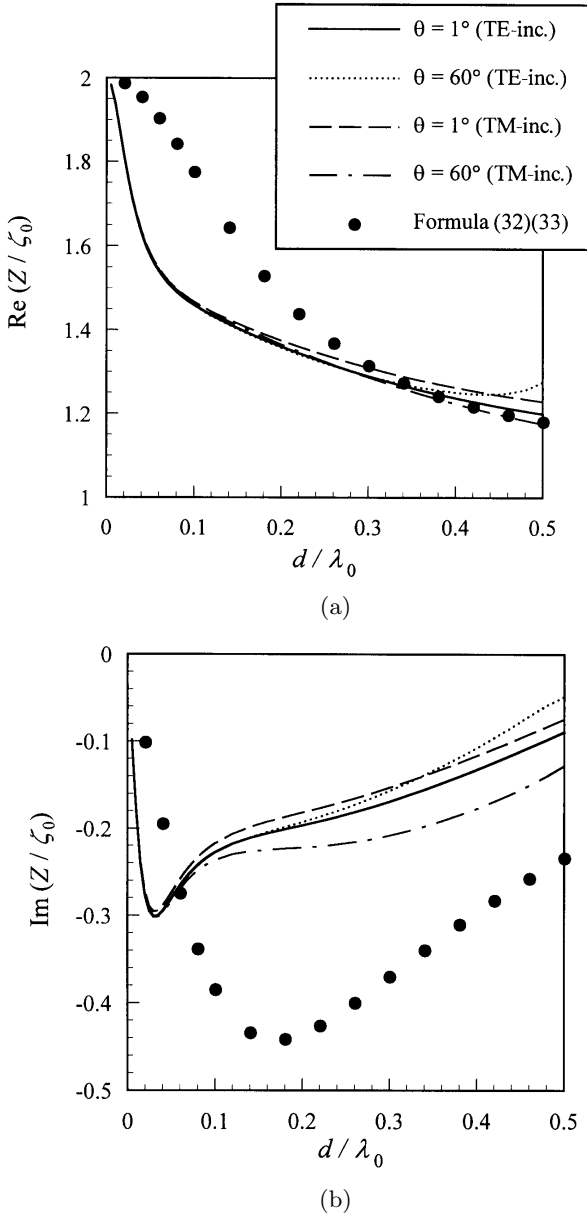


**Figure 8.** Frequency dependence of the equivalent impedance for the resistive grating. The parameters are  $Q = 2$ ,  $h/d = 0.01$ ,  $2w/d = 0.5$ ,  $R/\zeta_0 = 1$ , and  $\varphi = 1^\circ$ . (a) Normalized resistance, (b) Normalized reactance.

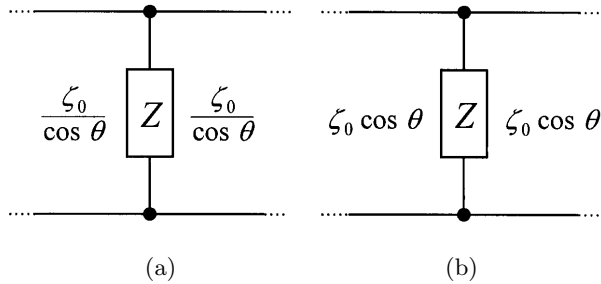


**Figure 9.** Equivalent circuit for plane resistive sheet or grating. (a) TE-incidence, (b) TM-incidence.

### 6. CONCLUSION

We have developed a numerical solution to the scattering problem with regard to crossed multilayered strip gratings. The moment method leads the problem into the set of linear equations, which is solved by carefully choosing the truncation numbers in order to avoid the ill convergence. Numerical computations were carried out to show the distribution of the incident power to the reflected, transmitted, and absorbed ones. The absorbing rate exceeds 94% by a proper choice of grating parameters. The equivalent circuit parameters of the crossed resistive grating were also obtained.

The treated structure is regarded as a microscopic model of electromagnetic wave absorbing sheet of the fiber type [8]. The knowledge of the equivalent parameters of the grating is useful in designing such absorbers. In view of applications, it is valuable to widen the absorbing range by admitting the strip width and periods to be unequal. Using multi-element gratings [13] seems another effective way. These problems deserve further attention.

### APPENDIX. EVALUATION OF INNER PRODUCT

The modal functions (8) and (18) are substituted into the definition of the inner product (21) and evaluated analytically. The result is arranged in the matrix form as

$$\begin{bmatrix} C_{1mn,1il}^{(p)} \\ C_{1mn,2il}^{(p)} \\ C_{2mn,1il}^{(p)} \\ C_{2mn,2il}^{(p)} \end{bmatrix} = \begin{cases} \delta_{nl} U_{ml}^{(1)} V_{ild} \begin{bmatrix} -j\alpha_i \beta_l w & m\pi \beta_l / 2 \\ j\beta_l^2 w & m\pi \alpha_i / 2 \\ -m\pi \alpha_i / 2 & j\beta_l^2 w \\ m\pi \beta_l / 2 & j\alpha_i \beta_l w \end{bmatrix} \\ \times \begin{bmatrix} \cos \frac{m\pi}{2} & -j \sin \frac{m\pi}{2} \\ -\sin \frac{m\pi}{2} & -j \cos \frac{m\pi}{2} \end{bmatrix} \begin{bmatrix} I_+ \left( \frac{m}{2}, \frac{\alpha_i w}{\pi} \right) \\ I_- \left( \frac{m}{2}, \frac{\alpha_i w}{\pi} \right) \end{bmatrix} \\ (p : \text{odd}) \\ \\ \delta_{mi} U_{in}^{(2)} V_{ild} \begin{bmatrix} j\alpha_i \beta_l w & -n\pi \alpha_i / 2 \\ j\alpha_i^2 w & n\pi \beta_l / 2 \\ n\pi \beta_l / 2 & -j\alpha_i^2 w \\ n\pi \alpha_i / 2 & j\alpha_i \beta_l w \end{bmatrix} \\ \times \begin{bmatrix} \cos \frac{n\pi}{2} & -j \sin \frac{n\pi}{2} \\ -\sin \frac{n\pi}{2} & -j \cos \frac{n\pi}{2} \end{bmatrix} \begin{bmatrix} I_+ \left( \frac{n}{2}, \frac{\beta_l w}{\pi} \right) \\ I_- \left( \frac{n}{2}, \frac{\beta_l w}{\pi} \right) \end{bmatrix} \\ (p : \text{even}) \end{cases} \quad (\text{A.1})$$

where

$$I_{\pm}(\xi, \eta) = \text{sinc}(\xi + \eta) \pm \text{sinc}(\xi - \eta) \quad (\text{A.2})$$

$$\text{sinc} \xi = \frac{\sin(\pi\xi)}{\pi\xi} \quad (\text{sinc } 0 = 1) \quad (\text{A.3})$$

## ACKNOWLEDGMENT

This work was supported by the 1999 award of the SUMMA Graduate Fellowship in Advanced Electromagnetics, USA.

## REFERENCES

1. Zinenko, T. L., A. I. Nosich, and Y. Okuno, "Plane wave scattering and absorption by resistive-strip and dielectric-strip periodic gratings," *IEEE Trans. Antennas Propagat.*, Vol. AP-46, No. 10, 1498–1505, 1998.
2. Matsushima, A., T. L. Zinenko, H. Minami, and Y. Okuno, "Integral equation analysis of plane wave scattering from multilayered

- resistive strip gratings," *J. Electromagn. Waves Applic.*, Vol. 12, No. 11, 1449–1469, 1998.
3. Zinenko, T. L., A. Matsushima, and Y. Okuno, "Scattering and absorption of electromagnetic plane waves by a multilayered resistive strip grating embedded in a dielectric slab," *IEICE Trans. Electron.*, Vol. E82-C, No. 12, 2255–2264, 1999.
  4. Senior, T. B. A., and J. L. Volakis, "Approximate boundary conditions in electromagnetics," *IEE Electromagnetic Waves Series*, 41, 1995.
  5. Lee, S. W., W. R. Jones, and J. J. Campbell, "Convergence of numerical solutions of iris-type discontinuity problems," *IEEE Trans. Microwave Theory Tech.*, MTT-19, No. 6, 528–536, 1970.
  6. Hill, D. A., and J. R. Wait, "Electromagnetic scattering of an arbitrary plane wave by two nonintersecting perpendicular wire grids," *Can. J. Phys.*, Vol. 52, 227–237, 1974.
  7. Krohn, T. L., and L. N. Medgyesi-Mitschang, "Scattering from composite materials: a first-order model," *IEEE Trans. Antennas Propagat.*, Vol. AP-37, No. 2, 219–228, 1989.
  8. Lin, M. S., and C. H. Chen, "Plane wave shielding characteristics of anisotropic laminated composites," *IEEE Trans. Electromagn. Compat.*, Vol. 35, No. 1, 21–27, 1993.
  9. Lee, S. W., G. Zarrillo, and C. L. Law, "Simple formulas for transmission through periodic metal grids or plates," *IEEE Trans. Antennas Propagat.*, Vol. AP-30, No. 5, 904–909, 1982.
  10. Vardaxoglou, J. C., *Frequency Selective Surfaces—Analysis and Design*, John Wiley, Research Studies Press Ltd., 1997.
  11. Braver, I. M., P. Sh. Fridberg, K. L. Garb, and I. M. Yakover, "The behavior of the electromagnetic field near the edge of a resistive half-plane," *IEEE Trans. Antennas Propagat.*, Vol. AP-36, No. 12, 1760–1768, 1988.
  12. Butler, C. M., "The equivalent radius of a narrow conducting strip," *IEEE Trans. Antennas Propagat.*, Vol. AP-30, No. 4, 755–758, 1982.
  13. Litvinenko, L. N., "Diffraction of electromagnetic waves at multi-element and multi-layer gratings," *Zhurn. Vychislit. Matem. i Matem. Fiziki.*, Vol. 10, No. 6, 1419–1446, 1970.